Life-Cycle of Structures and Infrastructure Systems – Biondini & Frangopol (Eds)

Hygro-thermo-chemo-mechanical coupled discrete model for the self-healing in Ultra High Performance Concrete

A. Cibelli, L. Ferrara & G. Di Luzio
Department of Civil and Environmental Engineering, Politecnico di Milano, Milan, Italy

ABSTRACT: Reliable durability predictions and design for advanced cement-based materials cannot disregard the modelling of their inherent self-healing capability. A discrete meso-scale model to simulate the recovery in water tightness, stiffness and strength induced by the (stimulated) autogenous healing of cracks for Ultra High Performance Concrete is presented. In this paper the model is implemented into the numerical framework of the Multiphysics-Lattice Discrete Particle Model (M-LDPM), resulting from the coupling of the Hygro-Thermo-Chemical (HTC) model and Lattice Discrete Particle Model (LDPM). Consistently with experimental evidence, the development of the self-repairing process is modelled as consisting of two independent stages: (a) the healing of matrix cracks, affecting both moisture permeability and fracture strength in the cracked state, and (b) the recovery in terms of fibre bridging action, relying on the adhesion between the healing products and the walls of the tunnel cracks which form during the fibre debonding process. This research activity is framed into the Horizon 2020 project ReSHEALience (GA 760824).

1 INTRODUCTION

Concrete cracks, even in service conditions, represent a predisposing factor for several degradation phenomena. As a consequence, in the last decades the comprehension of the processes affecting the concrete long-term performance has gathered an increasing interest among concrete professionals and researchers. Reliable durability predictions and design for either ordinary and/or advanced cementitious materials cannot disregard a proper modelling of their inherent self-healing capability. As demonstrated in a number of experimental works (e.g. Snoeck and De Belie 2015; Ferrara et al. 2018), the latter might lead to a significant recovery of physical and, in some cases, mechanical properties in the cracked state.

In structural concrete research, the term self-healing refers to the material capacity of repairing the damage in cracked state autonomously. Three major categories of concrete self-healing can be identified: (i) autogenous when the mixture composition only includes regular concrete constituents, (ii) stimulated autogenous when tailored constituents of akin chemical nature are employed to facilitate the process, and (iii) autonomic/engineered when the inclusion of specific additions, not normally employed as such, is used with the explicit purpose of favouring/activating the healing reactions.

From an accurate literature survey it stands out that, over the years, researchers have placed much more effort on the experimental investigation of the self-healing process, rather than on the modelling issues. As a matter of fact, only few models have been developed to simulate how mechanical performance of concrete are affected by the healing of cracks (Barbero et al. 2005, Voyiadjis et al. 2011, Aliko-Benítez et al. 2015, Hilloulin et al. 2016, Davies and Jefferson 2017, Oucif et al. 2018, Di Luzio et al. 2018, Jefferson et al. 2018, Yang et al. 2020, Chen et al. 2021). To the best of the authors' knowledge, none of them addresses the issue concerning the reduction of moisture permeability due to the autonomous cracks clogging. Furthermore, the majority of the published models relies on continuum-based

DOI: 10.1201/9781003323020-148

approaches, and consider the healing-induced effects on the mechanical properties as a smeared contribution in terms of stiffness and strength recovery in the cracked state. With this approach, they miss in simulating the local nature of the phenomena.

In this paper a discrete model to simulate the recovery in water tightness, stiffness and strength induced by the (stimulated) autogenous healing of cracks for Ultra High Performance Concrete is presented. The model is implemented into the numerical framework of the Multi-physics-Lattice Discrete Particle Model (M-LDPM) (Alnaggar et al. 2017), resulting from the coupling of the Hygro-Thermo-Chemical (HTC) model (Di Luzio and Cusatis 2009, Pathirage et al. 2019) with the Lattice Discrete Particle Model (LDPM) (Cusatis et al. 2011) and its extension to fibre-reinforced concrete (LDPM-F) (Schauffert and Cusatis 2012). Consistently with experimental evidence, the development of the self-repairing process is modelled as consisting of two independent stages: (a) the healing of matrix cracks, affecting both moisture permeability and fracture strength in the cracked state, and (b) the recovery in terms of fibre bridging action, relying on the friction between the healing products and the walls of the tunnel cracks which form during the fibre debonding process.

This research activity was framed into the Horizon 2020 project ReSHEALience, which was terminated in March 2022 and delivered two valuable results: (i) the concept of Ultra High Durability Concrete, articulated into a sound approach to tailor the mix design depending on the environmental conditions to face (Lo Monte and Ferrara 2020, Lo Monte and Ferrara 2021), and (ii) a Durability Assessment-based Design strategy, validated against laboratory evidences and on-site monitoring data (Al-Obaidi et al. 2021).

2 MODELLING APPROACH

The modelling approach herein presented can be classified as a multi-scale model, in which two different scales of damage phenomena are considered: (i) matrix cracks at the mesoscale, and (ii) fibre-matrix interface cracks, which are governed by mechanisms occurring at the microscale (Figure 1). In the following, the latter are also referred to as *tunnel* cracks.

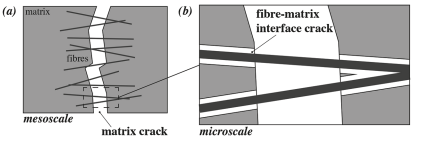

Figure 1. (a) matrix cracks at the mesoscale; (b) fibre-matrix interface cracks at the microscale.

The modelling approach relies on the idea for which the self-healing of matrix and tunnel cracks affect the material mechanical behaviour differently. For this reason, the autogenous repairing of the matrix cracks is implemented within the constitutive fracture law at the meso-scale, whereas the effect of healing on the fibres response is taken into account within the calculation of the bridging force carried by the discrete fibre reinforcement.

In the proposed model, the moisture permeability is assumed to be affected only by the matrix cracks, then only their closure contributes to the recovery in water-tightness that healed material might experience. The healing of the tunnel cracks has been considered to play a role exclusively on the mechanical behaviour.

3 NUMERICAL IMPLEMENTATION IN M-LDPM

3.1 *Evolution of the healing process*

The healing kinetic law formulated for plain cementitious materials (Di Luzio et al. 2018) can be employed for fibre-reinforced composites as well. Since the damage in the mechanical model evolves a two different scales (i.e. meso- and microscale), the implementation in the HTC module within the M-LDPM framework is performed by following the same conceptual

differentiation between matrix and tunnel cracks. This yields a two-fold advantage: (i) the possibility of having two separate internal variables describing the damage healing phenomena (i.e. λ_{sh}^{m} for matrix cracks and λ_{sh}^{f} for tunnel cracks) feeding the mechanical model at two different levels, and (ii) the chance of capturing the effect that the self-sealing of the matrix cracks has on the moisture permeability in the cracked state. In the following the formulation emphasising this differentiation is reported, with no theoretical differences with respect to the original one (Di Luzio et al. 2018).

Hereinafter the superscript k can be either m or f depending on which scale of damage is of interest. When $k = m$ formulas and parameters refer to the matrix cracks at the mesoscale, whereas with $k = f$ they refer to tunnel cracks at the microscale.

The kinetic laws reads

$$\dot{\lambda}_{sh}^{k} = \tilde{A}_{sh}^{k}\left(1 - \lambda_{sh}^{k}\right) \tag{1}$$

in which $\tilde{A}_{sh}^{k}$, inversely proportional to the reaction characteristic times, is calculated as

$$\tilde{A}_{sh}^{k} = \tilde{A}_{sh0}^{k} \cdot f_h(h) \cdot f_w^{k}(w_c) \cdot exp\left[-\frac{E_{sh}^{k}}{R}\left(\frac{1}{T} - \frac{1}{T_{ref}}\right)\right] \tag{2}$$

where $\tilde{A}_{sh.0}^{k}$, namely the inverse of the reaction characteristic times in standard conditions (RH=100%, $T = T_{ref}$, $w_c = 0$), values

$$\tilde{A}_{sh0}^{k} = \tilde{A}_{sh1}^{k}\left(1 - \alpha_c^{sh0}\right)c + \tilde{A}_{sh2}^{k} \cdot ad \tag{3}$$

where c and ad are the cement and healing-promoting admixture content, respectively. The material parameters E_{sh}^{k}, $\tilde{A}_{sh1}^{k}$, and $\tilde{A}_{sh2}^{k}$ are calibrated against experimental data, allowing to capture the key aspects of phenomena occurring at two different scales (Cibelli et al. 2022). In Eq. 2 the relative humidity, h, and temperature, T, fields are provided by the HTC model.

It is worth highlighting that the coefficient $f_w^{k}(w_c)$ provides the possibility of calibrating the effect of crack width on the process kinetic differently for matrix and tunnel cracks. Such double degree of freedom allows to trigger the healing model (i) at the mesoscale for cracks larger than the material macroporosity ($\approx 10 \div 20$ μm), and (ii) at the microscale for crack openings one order of magnitude smaller, as the debonding stage is typically characterised by narrower cracks.

The coefficient $f_h(h)$ accounts for relative humidity and simulates the relevant role played by the moisture supply, making the process proceed or stop whether the healing water-driven reactions are fed or not.

3.2 *Moisture permeability in the healed material*

The healing process has a significant effect on the moisture diffusion in presence of cracks due to the crack closure effect. This phenomenon is taken into account straightforwardly in the factor governing the crack size dependence of water permeability $f_D(w_c)$, whose formulation reads

$$f_D(w_c) = \frac{D_h^{cracked}(h, T, w_c)}{D_h^{uncracked}(h, T)} = 1 + \frac{999e^{n_c}\xi}{1 - (1 - e^{n_c})\xi} \tag{4}$$

in which $\xi = \min[\max(w_c - w_{c0}; 0)/w_{c1} - w_{c0}; 1]$, by replacing the crack opening w_c with $w_c \cdot (1 - \lambda_{sh}^{(m)})$. It means that the actual damage affecting the moisture permeability is reduced proportionally to the evolution of the self-healing process up to completion, i.e. $w_c \cdot \left(1 - \lambda_{sh}^{(m)}\right) = 0$ for $\lambda_{sh}^{(m)} = 1$. It is worth emphasising that $\lambda_{sh}^{(m)}$ assumes the meaning of matrix crack closure degree. w_{c0} and w_{c1} express two threshold values. When $w_{c0} \leq w_c \leq w_{c1}$, D_h and moisture transport phenomena undergo a sudden and steep increment, due to a material permeability up to 1000 times larger. For $w_c \geq w_{c1}$, instead, the moisture flux stops growing even though cracks continue widening.

3.3 *Self-healing of matrix cracks in LDPM*

The matrix cracks (Figure 1a) are induced by the loads, either mechanical or environmental, and are responsible of the fibres mechanical activation: as long as no cracks intersect a fibre, the latter does not contribute to the structural response.

For matrix cracks, the healing effect is modelled by enforcing a homothetic expansion of the LDPM boundary limit curve $\sigma_{bt}(\varepsilon,\omega) = \sigma_0(\omega)\exp[-H_0(\omega)\langle\varepsilon_{max} - \varepsilon_0\rangle/\sigma_0(\omega)]$, as more pronounced as more the repairing process has developed. Experimental evidences have confirmed that even plain concrete specimens, once loaded, fractured and unloaded, might show a recovery in strength and stiffness if re-loaded after a curing period in a moist environment. This is mainly due to two water-driven phenomena occurring in the cracks: delayed hydration and calcium carbonation precipitation. The healing products partially restore the material continuity, lowering, at least locally, the material bulk permeability and limiting the ingress of aggressive agents. The effect on the mechanical response, instead, depends on: (i) the chemical bounds between the filling products and the crack walls, and (ii) the nature, strength and stiffness of the healing products. Because of this, it is not granted that the crack sealing results in an actual concrete healing.

In this work, the modelling strategy adopted relies on the homothetic expansion of the boundary curve $\sigma_{bt}(\varepsilon,\omega)$ (Figure 2a) proportional to the healing degree λ_{sh}^{m}. Then, it allows to capture the recovery in strength, without varying the crack width within the numerical framework. Therefore, the healed material must be allowed to have a fracture strength exceeding that of the same material with the same level of damage with no healing occurred.

In LDPM, the healing implementation affects the strength limit calculation, thus, on turn, the limit curve. The updated version of the healing dependent-constitutive law relevant to the fracture behaviour reads

$$\sigma_0\left(\omega,\lambda_{sh}^{m}\right) = \sigma_0(\omega)\left(1 + c_{sh}\cdot\lambda_{sh}^{m}\right) \tag{5a}$$

$$\sigma_{bt}\left(\varepsilon,\omega,\lambda_{sh}^{m}\right) = \sigma_0\left(\omega,\lambda_{sh}^{m}\right) exp\left[-H_0(\omega)\frac{\langle\varepsilon_{max} - \varepsilon_0\rangle}{\sigma_0\left(\omega,\lambda_{sh}^{m}\right)}\right] \tag{5b}$$

In Eq. 5a, c_{sh} is an empirical coefficient steering the impact of crack closure on mechanical strength. It is defined as *healing mechanical impact coefficient*. The parameter c_{sh} depends on several aspects, e.g. curing conditions and mixture composition, therefore, it has to be calibrated experimentally. Looking at the updated equation of the boundary curve (Eq. 5b), it is important to notice that the healing, through the product $c_{sh}\cdot\lambda_{sh}^{m}$, governs the shape of the softening branch and sets the stress limit for the earlier stage of the constitutive law, namely when the maximum strain does not exceed the elastic limit. However, though the modelling strategy involves both linear and post-peak behavior, the former is never imposed at the mesoscale, being the limit curve expanded exclusively on those facets which experience cracking and healing.

3.4 *Self-healing of tunnel cracks in LDPM-F*

The fibre-matrix interface cracks (Figure 1b) develop during the interface debonding. Experimental evidences, collected through single-fibre pull-out tests, stopped after the first load drop and resumed up to rupture upon curing featuring different duration and exposure conditions (Qiu et al. 2019), confirmed that the healing of the interface cracks does affect the pull-out strength. As a matter of fact, whenever the healing process happens, delayed hydration products and $CaCO_3$ crystals fulfill the tunnel between the fibre and the surrounding mortar. This results in a recovery of the interface frictional bond. The phenomenon is implemented in LDPM-F by updating the value of the fibre bridging force $P(v)$ with a coefficient proportional to λ_{sh}^{f}. The updated constitutive law for the fibre load reads

$$P\left(v,\lambda_{sh}^{f}\right) = \left(1 + \gamma_{sh}\cdot\lambda_{sh}^{f}\right)P(v) \le \alpha\cdot P_0 \tag{6}$$

Referring to a single-fibre pull-out test, in Figure 2b the effect of the tunnel crack self-healing on the mechanical response is qualitatively shown. After the loading and unloading stages (branches L and U), the specimen is exposed to given environmental conditions for a time span long enough to permit the self-healing process to develop. The cured specimen is then reloaded (branch R) up to rupture. Due to the recovered frictional bond, the specimen might experience a recovery in stiffness and strength, to an extent proportional to the degree of completion of the healing process. By means of the device in Eq. 6, LDPM-F is updated to be capable of capturing this experimental evidence. In Figure 2b the updated constitutive law is plotted with reference to increasing self-healing degrees, in the hypothesis of $\gamma_{sh} = 1.00$.

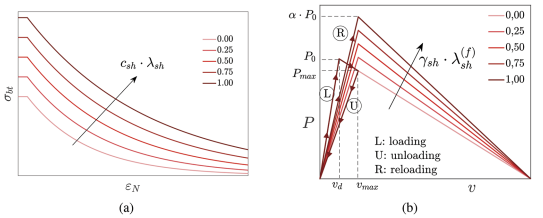

Figure 2. Healing model: (a) matrix cracks; (b) fibre-matrix interface (or tunnel) cracks.

The coefficient γ_{sh} has a physical meaning similar to c_{sh}. It governs the impact that the healing of the tunnel cracks has on the fibres contribution to the mechanical equilibrium. With $\gamma_{sh} = 0$ it is possible to capture the crack sealing, whereas if $\gamma_{sh} \geq 0$ the load carried by the fibre is enhanced thanks to the increased friction along the crack walls. The latter has an upper bound ($\alpha \cdot P_0$) in which the bridging force at full debonding P_0 is either amplified or reduced by the coefficient α. Both γ_{sh} and α are material parameters to calibrate against experimental data. Depending on the composition of the cementitious composites, the technique adopted to engineer the process, the type of the fibres (i.e. material, geometry), the curing conditions and the loading regimes, the healing might allow to recover either partially or entirely the fibre load bearing capacity. The parameter α sets the maximum achievable level of recovery. Once calibrated experimentally, γ_{sh} must comply with the condition for which, in case of full fulfilment of the tunnel crack:

$$\text{if} \quad \lambda_{sh}^{f} = 1.00 \Rightarrow \gamma_{sh} \leq \frac{\alpha \cdot P_0}{P(v)} - 1 \tag{7}$$

4 VALIDATION OF THE IMPLEMENTED MODEL

4.1 *Matrix cracks*

The model implementation is expected to affect the mechanical response of the material in tension and shear. In order to investigate the reliability of the implemented model, the numerical simulations of how two ordinary plain concrete (OPC) specimens behave after being damaged in tension and brought to collapse, after curing, either in pure tension or shear have been executed. The material adopted has been an ordinary plain concrete whose mix composition included: (i) cement (300 kg/m^3), (ii) water (190 kg/m^3), and (iii) aggregates 5.5 ÷ 16 mm (1950 kg/m^3).

The behaviour in tension has been investigated for a dogbone (DB) specimen, as usual for pure tensile tests, having the dimensions reported in Figure 3a and thickness of 20 mm. The dimensions have been chosen in order to localise the damage in the narrowest part of the sample, namely the mid-span cross-section. The other geometrical characteristics have been set accordingly. For the shear behaviour, instead, a double edge notched prismatic (DENP) specimen has been used (Figure 3b), having dimensions 100×70×20 mm^3, and the notches 2 mm wide and 25 mm deep. It has been necessary to avoid a slender sample, as the dog-bone specimen presented above is. As a matter of fact, a stocky element presents a larger proneness

to shear failure. For both specimens it has been necessary (i) to shape the sample in order to have all the mechanical energy channelled into the growth of the fracture at the mid-span, with no dispersion due to multi-cracking scenarios, and (ii) to have the smallest dimension larger than the maximum aggregate size of the simulated material.

Once the samples geometry has been generated, both specimens have been damaged by means of an increasing tensile loading, up showing a single crack roughly $350\mu m$ wide (Figures 3c,d). Afterwards, the dog-bone sample has been brought to failure in tension, whereas the one in shear. This second stage has been repeated after having imposed an increasing value of the normalised healing degree, λ_{sh}^{m}, ranging from 0.00 to 1.00, and in the hypothesis of having unit healing mechanical impact coefficient, c_{sh}. Then, in Figures 3e,f, the model ability of catching the healing-induced recovery in tensile and shear strength is shown plotting the (e) tensile load vs. displacement and (f) shear load vs. slip curves.

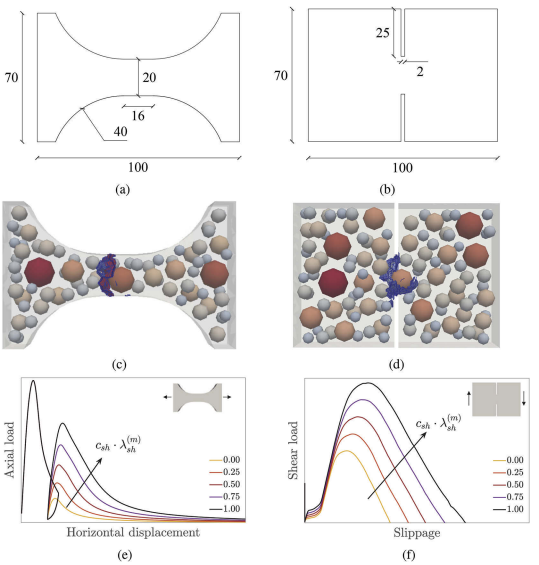

Figure 3. (a,b) DB and DENP dimensions in mm; (c,d) DB and DENP specimens: aggregate particles and cracks; (e,f) DB and DENP specimens: pure tension for pre- and re-cracking.

4.2 *Tunnel cracks*

The dogbone specimen in Figure 3a has been used also for testing the implementation of the tunnel cracks healing, by generating a FRC-based mesh with the same geometry. The concrete composition included: (i) cement (600 kg/m^3), (ii) water (200 kg/m^3), (iii) aggregates ranging between 3 ÷ 6 mm (1518 kg/m^3), and (iv) steel fibres with diameter and length equals to 0.22 mm and 20 mm, respectively (0.50% by volume).

As for matrix cracks, the purpose of investigating if the healing implementation affects the fibre load-slip constitutive law as expected is achieved through a simple set of numerical simulations. The dogbone specimen has been loaded in uniaxial tension up to feature a single prominent crack ($w_c \approx 60\,\mu m$). Then, it has been completely unloaded; afterwards, the sample has been reloaded up to failure. The reloading stage has been performed by assuming for λ_{sh}^{f} increasing fixed values: 0.00, 0.25, 0.50, 0.75, and 1.00. The numerical simulations have been carried out in two different scenarios: with no matrix cracks healing, $\lambda_{sh}^{m} = 0.00$, and in the hypothesis of matrix and tunnel cracks healing evolving identically, $\lambda_{sh}^{m} = \lambda_{sh}^{f}$.

Firstly, it is important to assess how the model performs at the single fibre-facet intersection. The comparison between the fibre load vs. slip curves on one of the most damaged LDPM facets obtained with λ_{sh}^{f} equals to 0.00 and 1.00 are shown in Figure 4b. The effect of healing acts as expected, though the re-loading in presence of healing stops before reaching

the ultimate slip (Figure 4b). As it stands out from Figure 4c, the numerical model is able to capture what has been experimentally observed in (19), where the authors detected a recovery in load-bearing capacity at macroscale with a negligible matrix crack healing. Finally, in Figure 4d, the model captures the coupled effect also on the fracturing behaviour induced by the simultaneous autogenous repairing of both matrix and tunnel cracks.

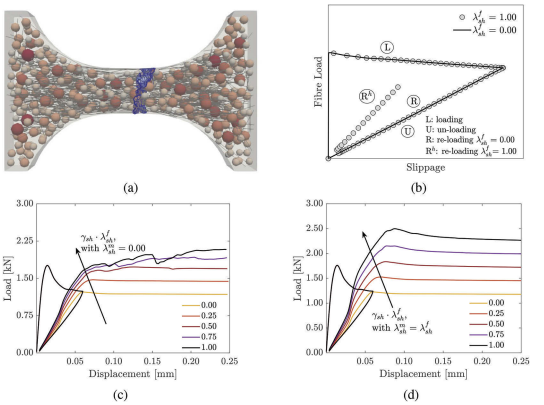

Figure 4. (a) DB FRC specimen: aggregate particles, fibres and cracks; (b) fibre load vs. slip curve experienced along one of the most damaged facets; (c) only tunnel cracks healing; (d) both matrix and tunnel cracks healing.

5 CONCLUSIONS

The model presented in this work has proved to have the potential for capturing phenomenological trends and mechanics standing out from the experimental investigations available in the literature.

The proposed numerical model presents a framework allowing to simulate the self-healing capacity of fibre reinforced cementitious composites, as affected by both the matrix crack sealing (i.e. reconstruction of material through crack continuity) and fiber-matrix interface crack healing, also called tunnel cracks, resulting into a recovery of the fibre-matrix bond capacity.

The validation against laboratory results, currently matter of study, might help in further improving the proposed approach.

ACKNOWLEDGMENTS

The work described in this paper has been performed in the framework of the Horizon 2020 project ReSHEALience (funded by European Commission, GA No 760824), whose funding the authors gratefully acknowledge. The information and views set out in this publication do not necessarily reflect the official opinion of the European Commission. Neither the European Union institutions and bodies nor any person acting on their behalf, may be held responsible for the use which may be made of the information contained therein. The numerical analyses have been performed by means of MARS, distributed by ES3 Inc. (Engineering and Software System Solutions), which is gratefully acknowledged.

REFERENCES

Al-Obaidi, S., Bamonte, P., Animato, F., Lo Monte, F., Mazzantini, I., Luchini, M., Scalari, S. and Ferrara, L. 2021. Innovative design concept of cooling water tanks/basins in geothermal power plants using ultra-high-performance fiber-reinforced concrete with enhanced durability. *Sustainability* 13(17): 9826.

Aliko-Benítez, A., Doblaré, M. and Sanz-Herrera, J. 2015. Chemical-diffusive modeling of the self-healing behavior in concrete. *Int. J. of Sol. and Struct*. 69–70:392–402.

Alnaggar, M., Di Luzio, G. and Cusatis, G. 2017. Modeling time-dependent behavior of concrete affected by alkali silica reaction in variable environmental conditions. *Materials* 10(5): 471.

Barbero, E. J., Greco, F. and Lonetti, P. 2005. Continuum damage-healing mechanics with application to self-healing composites. *Int. J. of Dam. Mech*. 14(1): 51–81.

Chen, Q., Liu, X., Zhu, H., Ju, J. W., Yongjian, X., Jiang, Z. and Yan, Z. 2021. Continuum damage-healing framework for the hydration induced self-healing of the cementitious composite. *Int. J. of Dam. Mech*. 30(5): 681–699.

Cibelli, A., Pathirage, M., Ferrara, L., Cusatis, G. and Di Luzio, G. 2022. A discrete numerical model for the effects of crack healing on the behaviour of ordinary plain concrete: Implementation, calibration, and validation. *Eng. Frac. Mech*. 263: 108266.

Cusatis, G., Pelessone, D. and Mencarelli, A. 2011. Lattice discrete particle model (LDPM) for failure behavior of concrete. I: Theory. *Cem. and Con. Comp*. 33(9): 881–890.

Davies, R. and Jefferson, A. 2017. Micromechanical modelling of self-healing cementitious materials. *Int. J. of Sol. and Struct*. 113–114:180–191.

Di Luzio, G. and Cusatis, G. 2009a. Hygro-thermo-chemical modeling of high-performance concrete. I: Theory. *Cem. and Con. Comp*. 31(5): 301–308.

Di Luzio, G., Ferrara, L. and Krelani, V. 2018. Numerical modeling of mechanical regain due to self-healing in cement based composites. *Cem. and Con. Comp*. 86: 190–205.

Ferrara, L., Van Mullem, T., Alonso, M. C., Antonaci, P., Borg, R. P., Cuenca, E. A., Jefferson, A., Ng, P. L., Peled, A., Roig, M., Sanchez, M., Schroefl, C., Serna, P., Snoeck, D., Tulliani, J. M. and De Belie, N. 2018. Experimental characterization of the self-healing capacity of cement based materials and its effects on the material performance: a state of the art report by COST Action SARCOS WG2. *Constr. and Build. Mat*. 167: 115–142. Amsterdam: Elsevier.

Hilloulin, B., Hilloulin, D., Grondin, F., Loukili, A. and De Belie, N. 2016. Mechanical regains due to self-healing in cementitious materials: Experimental measurements and micro-mechanical model. *Cem. and Con. Res*. 80: 21–32.

Jefferson, A., Javierre, E., Freeman, B., Zaoui, A., Koenders, E. and Ferrara, L. 2018. Research Progress on Numerical Models for Self-Healing Cementitious Materials. *Adv. Mat. Interf*. 5: 1701378.

Jefferson, A. and De Belie, N. 2016. Mechanical regains due to self-healing in cementitious materials: Experimental measurements and micro-mechanical model. *Cem. and Con. Res*. 80: 21–32.

Lo Monte, F. and Ferrara, L. 2020. Tensile behaviour identification in ultra-high performance fibre reinforced cementitious composites: indirect tension tests and back analysis of flexural test results. *Mat. and Struct*. 53(6):145. Berlin: Springer.

Lo Monte, F. and Ferrara, L. 2021. Self-healing characterization of UHPFRCC with crystalline admixture: Experimental assessment via multi-test/multi-parameter approach. *Constr. and Build. Mat*. 283: 122579. Amsterdam: Elsevier.

Oucif, C., Voyiadjis, G. Z. and Rabczuk, T. 2018. Modeling of damage-healing and nonlinear self-healing concrete behavior: Application to coupled and uncoupled self-healing mechanisms. *Th. and Ap. Fract. Mech*. 96: 216–230.

Pathirage, M., Bentz, D., Di Luzio, G., Masoero, E. and Cusatis, G. 2019. The ONIX model: a parameter-free multiscale framework for the prediction of self-desiccation in concrete. *Cem. and Con. Comp*. 103: 36–48.

Qiu, J., He, S., Wang, Q., Su, H. and Yang, E. 2019. Autogenous healing of fiber/matrix interface and its enhancement. In G. Pijaudier-Cabot, P. Grassl and C. La Borderie (Eds.), *10th Int. Conf. on Fracture Mechanics of Concrete and Concrete Structures – FraMCoS-X, Bayonne, France,* 24–26 June 2019.

Schauffert, E. A. and Cusatis, G. 2012. Lattice Discrete Particle Model for fiber-reinforced concrete. I: Theory. *J. of Eng. Mech*. 138(7): 826–833.

Snoeck, D. and De Belie, N. 2015. From straw in bricks to modern use of microfibers in cementitious composites for improved autogenous healing – a review. *Constr. and Build. Mat*. 95: 774–787.

Voyiadjis, G. Z., Shojaei, A. and Li, G. 2011. A thermodynamic consistent damage and healing model for self healing materials. *Int. J. of Plast*. 27(7): 1025–1044.

Yang, S., Aldakheel, F., Caggiano, A., Wriggers, P. and Koenders, E. 2020. A Review on Cementitious Self-Healing and the Potential of Phase-Field Methods for Modeling Crack-Closing and Fracture Recovery. *Materials* 13(22): 5265.